Analysis of the Hygrothermal Environment in High-insulation Houses Using Stand-type Radiation Panel System

Lee Myonghyang[1], Akihito Ozaki[2], Yosuke Chiba[3], and Tadasu Ohishi[3]

1 Associate Professor, Institute of Science and Engineering, Ritsumeikan University, Ph D.,
Noji-higashi, Kusatsu, Shiga, 525-5877, Japan
2 Professor, Faculty of Human-Environment Studies, Kyushu University, Dr. Eng.,
Hakozaki, Fukuoka, 812-8581, Japan
3 Asahi Kasei Homes Corporation R&D Laboratories, Fuji, Shizuoka, 416-0934, Japan

ABSTRACT

In recent years, the demand for a highly efficient and comfortable hygrothermal environment has increased. Residential air conditioning using a system based on forced convection is prevalent in Japan. However, there are several problems associated with this type of system, such as unbalanced indoor temperature distribution, discomfort due to airflow, and diffusion of house dust. In addition, this system might also cause discomfort to the occupants, such as overcooling in the summer and excessive drying in the winter. An alternative is the radiation cooling/heating system, an air conditioning system that is already popular in Europe. This system is also being introduced into houses in Japan through mechanisms such as floor radiant heating. However, these systems tend not to be widely used due to unknown characteristics such as the delay in achieving the desired temperature, dehumidification due to condensation, and the radiant heat of the panel. In this study, we analyze indoor radiant heat and humidity characteristics using a stand-type radiation cooling/heating panel system installed in a highly insulated house. The characterization is performed using real-time measurements as well as numerical simulation. By using THERB for HAM (a residential building thermal environment simulation program for analyzing heat and moisture transfer), it is possible to predict the hygrothermal environment and the heat load of an entire building. We incorporate the algorithms for computing the parameters of the radiation panel system (heat convection, heat radiation, and two-dimensional heat conduction) in this simulation software.

INTRODUCTION

Currently, air conditioning systems based on forced convection are most widely used for heating and cooling indoor air in Japan. However, there are some issues associated with this method, including discomfort due to the directional airflow, the distribution of temperature, and the system noise (Watanabe et al., 2004). In order to address these issues, radiation cooling/heating systems are being studied and developed as an alternative to realize a high-quality indoor hygrothermal environment. At the same time, the radiation cooling / heating system is expected to have an energy-saving effect because it is possible to use a low-grade heat source.

In past research, dynamic analysis of the radiation panel system has been studied using CFD analysis or office

Figure 1 Appearance of the experimental house (Left)
Figure 2 Stand-type radiation panel (Right)

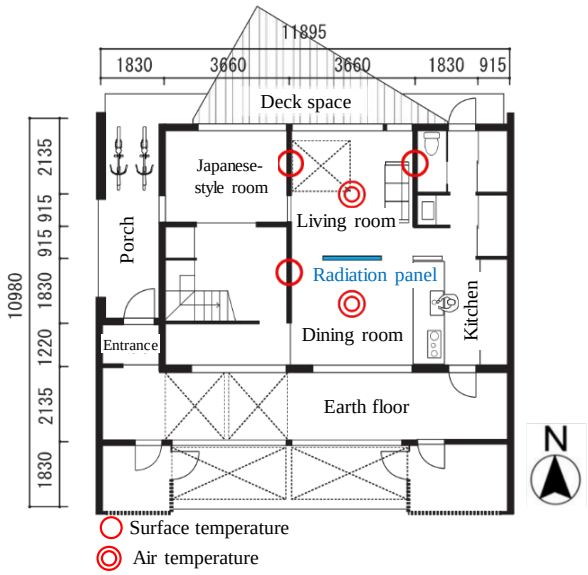

（1）First floor

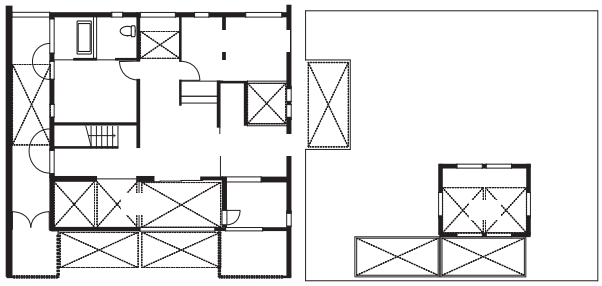

（2）Second floor *（3）Third floor*

Figure 3 Floor plan

Table 1 Equipment specification of the heat pump

Cooling capability	[kW]	3.0
Energy consumption	[kW]	1.2
Energy consumption efficiency	[-]	2.5
Range of water temperature	[°C]	7-25
Maximum water amount	[L]	30

Table 2 Building structure specifications

	Materials	Thickness [mm]		Materials	Thickness [mm]
Foundation	Polystyrene foam insulation	80	Earthen floor	Mortar	20
	Concrete	160		Phenol foam insulation	65
Ex-wall	Plaster board	12		ALC board	100
	Air space	27	Floor	Wooden floor	13
	Plywood	12		Plywood	12
	Phenol foam insulation	75		Mortar	20
	ALC board	75	Roof	ALC	100
In-wall	Plaster board	12		Phenol foam insulation	65
	Air space	100		Polystyrene foam insulation	25
	Plaster board	12		PVC waterproof sheet	2

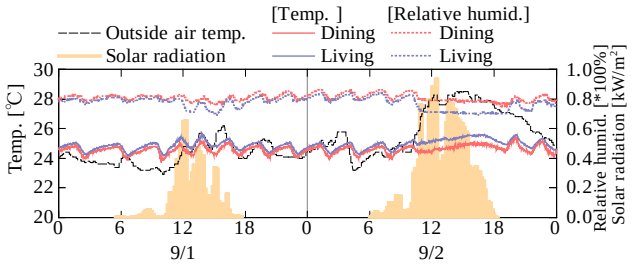

Figure 4 Indoor temperature

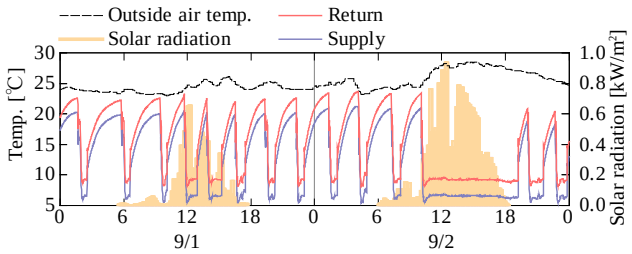

Figure 5 Water temperature in the radiation panel

environment experiments (Shioya, M et al., 2013. and Kim, J. et al., 2013.). However, a non-stationary analysis of radiation panel performance in a house has not been found. Further, studies that examined the net dehumidification from dew condensation on the radiation panel surface in summer have not been found.

The purpose of this study is to analyze the hygrothermal environment of a highly insulated house using a stand-type radiation cooling/heating panel system. In order to implement this, stand-type radiation panels were installed at a test house and parameters such as the room temperature, humidity, and energy consumption were monitored in the summer season. The conventional calculation method of radiation panel is estimated large heat transfer from panel surfaces because using the overall heat transfer coefficient and assuming that the temperature of supply water is constant by taking it as given that piping portion is layered. In this study, we also examine the revised calculation models (heat convection, heat radiation, and two-dimensional heat conduction) associated with the radiation panel system. We investigated the accuracy of the simulated values by comparing with measurement results. Furthermore, we analyzed the influence of the driving control method, water supply temperature, and number of panel sheets on the hygrothermal environment.

MEASUREMENT OF INDOOR ENVIRONMENT

Setup of the experimental building

As shown in Figure 1, an experimental steel-frame three-story house, with a total floor area of 172.87 m^2, was constructed in Fuji City, Shizuoka Prefecture. The stand-type radiation panel used in this study is shown in Figure 2. The floor plan of the building, measurement points, and position of the radiation panel are shown in Figure 3. The radiation panel is a slotted vertical panel; two such panels are placed between the living and dining rooms on the first floor. Including clearance, the width, height, and depth of the radiation panel are 898 mm, 2,441 mm, and 150 mm, respectively. The area of each radiation area is 2.19 m^2. The heat loss coefficient of the experimental house is 1.90 $W/(m^2 \cdot K)$. The house meets Japan's next generation energy conservation standards The heat pump and building specifications are listed in Table 1 and Table 2, respectively.

Measurement parameters and conditions

For two days (September 1 and 2, 2015), we measured the following parameters: external temperature, room temperature of each room, surface temperature of the walls in the main room, water temperature in the emission pipes going to and coming from the air-conditioning panel, and the panel surface temperature. The temperature of the emission air-conditioner was set to 26 °C and it was operated all day. In addition, there was no movement of people, no ventilation, and the blinds were not used during the survey period. The supply water temperature was 7 °C with a flow rate of 6 L/min.

Measurement results

Figure 4 shows the measured temperature and humidity of the living and dining rooms. The temperature of the living and dining rooms remained in the range of 25 °C to

26 °C when the radiation panel system was running. The measurement period was in September; therefore, the external temperature did not increase significantly. It was also observed that the air conditioner repeatedly started and stopped on September 1 because of the low amount of solar radiation. The relative humidity of the living and the dining rooms decreased when the radiation panel system was running.

Figure 5 shows the temperature of water in the emission pipes going to and coming from the air-conditioning panel. The supply water temperature was 7 °C during operation. Cold water was supplied continuously on September 2 because the amount of solar radiation increased, leading to a higher external temperature.

The temperature of water in the return pipes was about 9 °C. Thus, there was an approximate temperature difference of 2 °C between the pipes going in and returning. Consequently, it can be concluded that the heat radiated into the room.

NUMERICAL SIMULATION USING RADIATION PANEL

Simulation software of whole building

THERB for HAM (Ozaki et al., 2005) is a software package used to analyze the thermal environment of the whole building. This tool calculates the heat, moisture transfer, and airflow in a building based on the heat conduction, convection, and radiation associated with the physics of the building. Thus, it can predict the thermal environment and heat load in a room depending on the building specifications and other parameters such as the indoor heat and moisture. To this package, we added the algorithm used for calculation the radiant panel parameters.

Outline of radiation panel

A schematic diagram of the radiation-cooling panel is shown in Figure 6 (left: overall view of the panel, right: photo of the cooling surface of the panel (fin) and pipe). The placement of the heat dissipation area with respect to the living and dining rooms is shown in Figure 7. In each sheet panel, the fins are arranged in sixteen intervals of 50 mm. A single fin unit consists of two pipes of return tubes and forward pipes. The time-varying characteristics of convective heat transfer coefficients, nonlinearity of radiation heat transfer rates, and multiple reflections are taken into account in our calculation. These parameters come into play when the temperature of the panel surface changes. Half of the total surface area of the radiation panel is calculated assuming the area of heat transfer by convection and radiation to the cooling target chambers.

Method for calculating the radiation panel characteristics

(1) Convective heat transfer

Immediately after the radiation-cooling operation, a convective heat transfer occurs depending on the lowering or rising of the surface temperature. This change decreases as the system approaches the steady state.

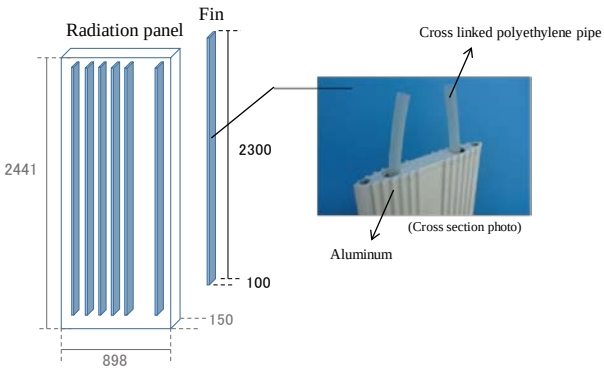

Figure 6 Schema of the radiation panel

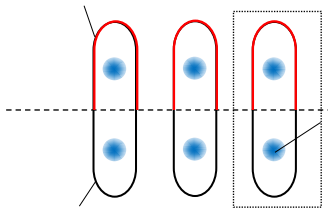

Figure 7 Heat radiation area

Natural convection heat transfer, with respect to the inner surface, is calculated from each and divided into horizontal and vertical planes, which are represented by dimensionless organized equations(Ozaki et al., 1990).

·Horizontal plane

$$Nu = C \cdot Ra_f^m \quad (1)$$

$$Ra_f = Gr_i \cdot Pr \quad (2)$$

$$f = (T_s + T_\infty)/2 \quad (3)$$

·Vertical plane

$$Nu = 0.241(Gr_i \cdot Pr) \quad (4)$$

$$Gr_i = g\beta\Delta T_a l^3/v^2 \quad (5)$$

Where the coefficient C and index m of equation (1) are as follows:

・Upswing heat flax

$C = 0.58, \quad m = 1/5 \quad (2 \times 10^7 < Ra_f)$

・Downward heat flax

$C = 0.54, \quad m = 1/4 \quad (2 \times 10^4 < Ra_f < 8 \times 10^6)$

$C = 0.15, \quad m = 1/3 \quad (8 \times 10^6 < Ra_f < 10^{11})$

The convection heat transfer rate α_c is calculated from Nusselt number Nu by equation (6).

$$\alpha_c = \frac{Nu \cdot \lambda}{l} \quad (6)$$

(2) Mutual emission between the indoor surfaces

As the difference between the indoor surface temperature and the air temperature increases immediately after the radiation cooling operation, it is difficult to predict the actual phenomenon that leads to radiant heat transfer. We use the air temperature and the overall heat transfer obtained by superimposing convective heat transfer as a

reference. We use the method of mutual radiation heat exchange between the indoor surfaces with the Gebhart absorption coefficient (Gebhart, 1959) in our calculation (see Figure 8).

The ratio of net long wave emission from surface *l* that is absorbed by surface *j* is defined in equation (7) using the long wave emission absorption coefficient $\beta_{l,j}$.

$$\beta_{l,j} = F_{l,j}\varepsilon_j + \sum_{k=1}^{J} F_{k,k}(1-\varepsilon_k)\beta_{k,j} \tag{7}$$

Therefore, the net amount of radiation by surface *j* is given in equation (8).

$$ELR_j = \varepsilon_j \sigma T_j^4 - \sum_{k=1}^{J} \beta_{k,j}\varepsilon_k \sigma T_k^4 S_k/S_j \tag{8}$$

Equation (8) can be transformed to equation (11) using the conservation law of energy and reciprocity theorem.

$$\sum_{k=1}^{J} \beta_{j,k} = 1 \tag{9}$$

$$\varepsilon_k S_k \beta_{k,j} = \varepsilon_j S_j \beta_{j,k} \tag{10}$$

$$\begin{aligned} ELR_j &= \varepsilon_j \sigma \sum_{k=1}^{J} \beta_{j,k}\left(T_j^4 - T_k^4\right) \\ &= \sum_{k=1}^{J} \beta_{j,k}\alpha_{r,jk}\left(T_j - T_k\right) \end{aligned} \tag{11}$$

Where $\alpha_{r,jk}$ is the radiation heat transfer coefficient from surface *j* to surface *k* and is approximated by equation (12).

$$\alpha_{r,jk} = 4\varepsilon_j \sigma\left\{\left(T_j + T_k\right)/2\right\}^3 \tag{12}$$

By applying the long wave absorption coefficient, heat generation by radiant heating/cooling can be divided into convection and long wave radiation.

The absorption amount ALR_j of the surface *j* is expressed by equation (13), assuming that the long wave radiation component is uniformly spread from the building division element of the building input model.

$$\begin{aligned} ALR_j &= \sum_{c=1}^{C} \frac{\beta_{c,j} LI_c S_c}{S_j} + \sum_{f=1}^{F} \frac{\beta_{f,j} LI_f S_f}{S_j} \\ &= \varepsilon_j \left(\sum_{c=1}^{C} \beta_{j,c} LI_c/\varepsilon_c + \sum_{f=1}^{F} \beta_{j,f} LI_f/\varepsilon_f \right) \end{aligned} \tag{13}$$

Therefore, the net radiation amount NLR_j of the surface *j* can be calculated by equation (14).

$$NLR_j = ELR_j - ALR_j \tag{14}$$

(3) Tow-dimensional heat transfer by fin efficiency

Figure 9 shows the internal configuration of the radiation panel (sectional view). Since the area between the two pipes in a fin unit exhibits two-dimensional heat transfer, we calculate the two-dimensional heat flow using the fin

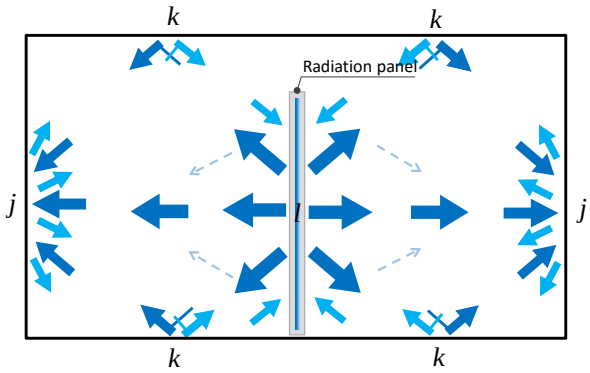

Figure 8 Multiple reflection of long wave radiation

efficiency. The conventional calculation method employing fin efficiency ignores the heat balance of piping the supply water portion and the piping part sets the pipe surface temperature as a virtual value. THERB assumes the piped supply water portion and the piping part to be the heat balance site, and it introduces fin efficiency to basic equations of heat and moisture conduction. In other words, the amount of heat supply for the hot and cold water is calculated by correcting and introducing fin efficiency in the thermal equilibrium equation. The supply of hot and cold water to the pitch part is computed by considering the effect of the hot and cold water layer on the heat balance of the panel.

The fin efficiency, which refers to the ratio of actual heat transfer from the fin surfaces to hypothetical heat transfer (assuming that the fin temperature is equal to the temperature of supply water in a tube), is applied to the radiation panel system. Equations (15) to (22) show the formulae used to calculate the fin efficiency.

·Fin efficiency

$$\eta_f = \frac{1}{w}\left[D + (w-D)\frac{\tanh mD}{mD}\right] \tag{15}$$

$$mD = \sqrt{\frac{C_f \cdot P}{\lambda_f \cdot t}}D \tag{16}$$

·Heat transmission coefficient from supply water to the tube surface

$$K_p = \frac{A_f}{L_f \cdot R_b} \tag{17}$$

$$R_b = \frac{D}{\lambda_w \cdot Nu} \tag{18}$$

$$Nu = \frac{0.0395 \cdot Re^{0.75} \cdot Pr}{1.+\left(1.99 \cdot Re^{-0.125} \cdot (Pr-1.0)\right)} \tag{19}$$

·Heat balance of supply water

$$C_w \cdot \rho_w \cdot V_w \frac{\partial T}{\partial t} = \eta_f \cdot K_p \cdot (T_m - T_w) \cdot L_f + Q_s \tag{20}$$

$$Q_s = q_f \cdot C_w \cdot \rho_w \cdot (T_{ws} - T_w) \tag{21}$$

$$\begin{aligned} -\frac{\partial T}{\partial t} &= \eta_f \cdot K_p \cdot (T_m - T_w) \\ &= \frac{1}{R_m} \cdot (T_m - T_{m-1}) + \frac{1}{R_{m+1}} \\ &\quad \cdot (T_m - T_{m+1}) \end{aligned} \tag{22}$$

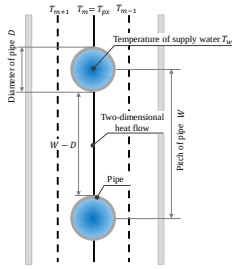

Figure 9 Inner structure

(4) Dew condensation of the panel

The influence of dew condensation induced by the radiation panel on the hygrothermal conditions is calculated by THERB using heat and moisture transfer principles based on the P-model utilizing the water potential (Ozaki, 2007). The P-model is defined using non-equilibrium thermodynamics, which has the theorem of conservation of energy and moisture. The water potential obtained by applying the chemical potential of thermodynamics to moisture diffusion is used as the driving force behind moisture transfer. The amount of dew condensation is calculated by multiplying the difference between the panel's unsaturated water potential and the room air's water potential by the moisture transfer rate of the panel.

Calculation accuracy

Table 3 shows the parameter values used in the calculation. The calculation was performed using data captured over two days, September 1 and 2, 2015. To reproduce the experimental conditions, the measured value per hour was used for weather conditions and the measured value per minute was used for supply-water temperature and velocity. The temperature of the emission air-conditioning was set to 26 °C, and the ventilation amount was set to nil, as there was no movement of people during this period. Figure 10 shows the calculated values for the temperature of the dining room, water temperature in the return pipe of the radiation panel, surface temperature of the panel, and the amount of load for the two days. The calculated values of the indoor temperature, cold-water return temperature, and panel surface temperature are comparable to the actual values.

However, the calculated value of the return pipe water temperature at the time that cooling was stopped was higher than the actual value. This is because we did not take into account the mutual radiation between the fin units in the calculation. The computed value was also more influenced by the room temperature than the measured value. With respect to the amount of load, the calculated and measured values almost match.

RADIATION PERFORMANCE OF RADIATION PANEL

Calculation conditions

Table 4 shows the parameter values used in the calculation. Table 5 and Table 6 present the cases considered in evaluating the radiation panel performance and the building performance. The weather conditions for a standard year at Shizuoka are shown in Figure 11. The conditions of the supply water are the same as the experiment conditions. In this study, we attempt to identify the sensitivity of the performance to radiation panel parameters and building specifications.

The influence of the driving control method, water supply temperature, and number of panel sheets on the indoor temperature is analyzed as shown in Table 5. The parameters of the radiation panel that are varied are as follows: control conditions of cold water (Case 1: natural

Table 3 Calculation conditions

Calculation period	9.1. - 9.2.2015
Weather conditions	Measured value per hour
Room temperature setting	26 °C
Amount of ventilation	-
Supply-water temperature	Measured value per minute
Supply -water velocity	

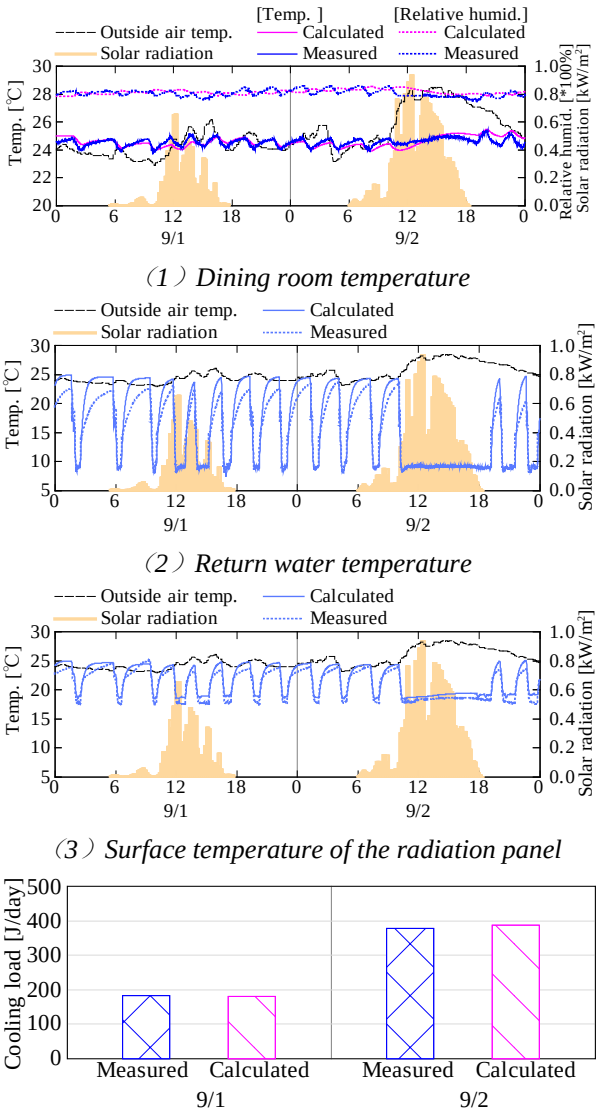

（1）Dining room temperature

（2）Return water temperature

（3）Surface temperature of the radiation panel

（4）Cooling load of integration value per day

Figure 10 Comparison of the calculated and actual value

state, Case 2: all-day operation, Case 3: 26 °C control), cold water temperature (Case 3: 12 °C, Case 4: 7 °C), and panel number (Case 3: 2 sheets, Case 5: 1 sheet, Case 6: 3 sheets). The building specifications for a change in panel performance are the same as those measured in the house (See Table 2).

The influence of building specification is analyzed as shown in Table 6. In this analysis, the control of the radiation panel is on-off control, the supply water temperature is 7 °C, and the number of panels is one. The difference in the performance of the insulation of the wall

Table 4 Calculation condition (stander parameter)

Calculation terms	2015.7.1～9.30
Calculation region	Shizuoka
Ventilation	Nothing
Flow rate of supply water	6 L/min
Preliminary calculation	5 days

Table 5 Calculation cases for the radiation panel

	Control of radiation panel	Supply water temp.	Number of panels
Case 1	Nothing	-	-
Case 2	All day	12 °C	2
Case 3	On-Off control of cold water at room temperature above 26 °C		
Case 4		7 °C	2
Case 5		12 °C	1
Case 6			3

Table 6 Calculation cases for the building performance

	Ex wall	Glazing	Blind
Case 7	GW16K 100 mm	Double glazing	Nothing
Case 8	Standard specification		
Case 9		Standard specification	Inner
Case 10			Outer

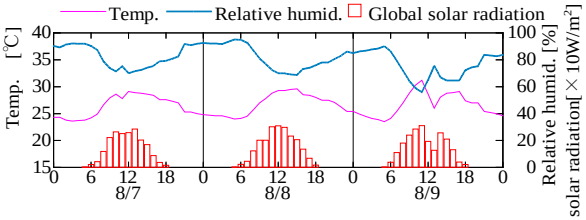

Figure 11 Weather data for Shizuoka

and windows, as well as the methods for blind use, are analyzed. The standard specification described in Table 6 are the same as those for the measured house.

Influence of radiation panel performance

Figure 12 shows the changes in the temperature and the frequency distribution of the living room temperature over three months (July 1 to September 30, 2009) using air conditioning for different values of the control method, cold water temperature, and number of panels. The natural state (Case 1) maintained an indoor temperature in the range of 26.5 °C to 27.9 °C. The all-day operation (Case 2) varied in the same manner, maintaining an indoor temperature approximately 1.5 °C lower than that of the natural state (Case 1). This is because of the cooling capacity of the radiant panel. In the case where the control was maintained at 26 °C, the room temperature was significantly affected by the number of panels (area).

A distribution in living room temperature at the time of air conditioning operation, even at 28 °C, appeared in the case of one panel (Case 5). In terms of the cold water temperature, the maximum value of the room temperature difference at the time of air conditioning operation at 12 °C (Case 3) and 7 °C (Case 4) was approximately

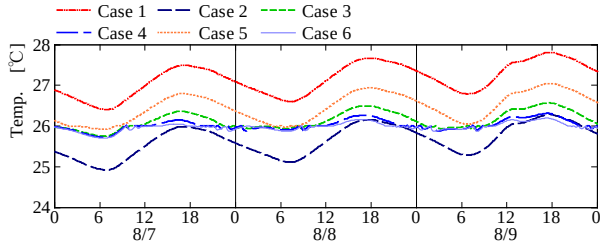

（1）Living room temperature

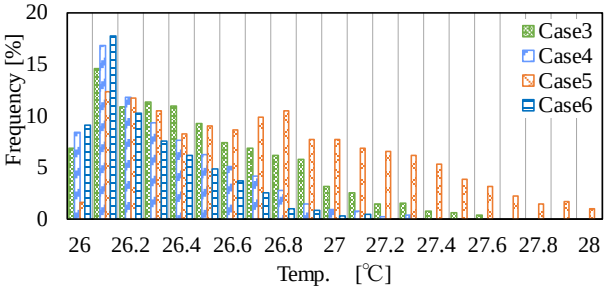

（2）Frequency distribution of Living room temperature during operation of the radiation panel

Figure 12 Effect of the radiation panel

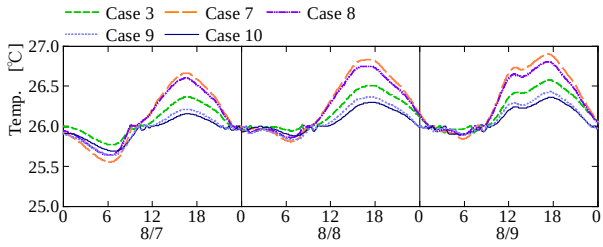

（1）Living room temperature

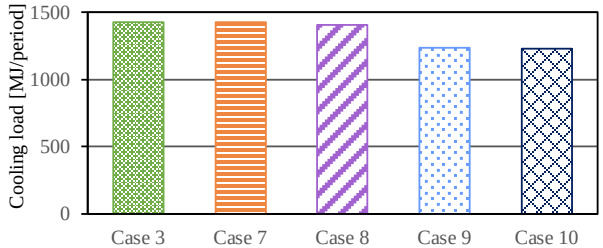

（2）Cooling load (July to Sep.)

Figure 13 Effect of the building performance

0.4 °C and no significant variation was observed.

Therefore, the radiation cooling is considered to have a sufficient cooling capacity with a low-grade heat source if the panel area is secured. In terms of the flow rate, the living room temperature for a rate of 5 L/min (Case 7) increased by approximately 0.2 °C when compared with the 3 L/min (Case 3). This is because the supplied cold

water was sent to the return tubes before sufficient heat dissipation could take place.

Influence of building specifications

Figure 13(1) shows the changes in the living room temperature with respect to changes in the building specification and the blinds over three days. In the case of the variation in the exterior wall (Case 7, Case 8), even if the radiation panel is operating, the room temperature rises by the outdoor air load. Moreover, the room temperature in Case 7 and Case 8 are comparable because the influence of the window is larger than that of the exterior wall. In the case of variation in the blinds setting (Case 9, Case 10), there are few changes in the room temperature when the radiation panel system is operating. It is possible that the outer blind (Case 10) shields the solar heat and efficiently conditions the room to maintain the temperature set by the radiation panel.
Figure 13(2) shows the cooling load during the summer (July to September). The heat load of Case 9 and Case 10, in which the blind is set up, decreased from that of the reference case (Case 3). The influence of heat shielding by the blind has a larger influence than the heat insulation because the window area is approximately 80% of the building envelope area.

HYGROTHERMAL ENVIRONMENT OF RADIATION PANEL

Calculation conditions

Dew condensation occurs on the radiation panel surface during radiation cooling in Japan. Therefore, the indoor thermal environment can be accurately predicted by calculating the amount of dew condensation on the panel. Table 7 shows the parameters used in the calculation. The results obtained using the air conditioner and the cooling radiation panels are compared. The indoor humidity calculation of the air conditioner is not assumed. The radiation panel calculations take into consideration the influence of indoor humidity with or without the dew condensation. The ventilation is taken as 0.5 times/h.

Influence of dew condensation

Figure 14 shows the indoor temperature, humidity, and the amount of dew condensation for each of the conditions. In the case of the air conditioner (Case A), the relative humidity is above 85%. Moreover, without the dew condensation calculation, both Case A and Case B exhibit fluctuations in the high humidity range. When the cold water temperature is 7 °C (Case C), the condensation amount is approximately twice of that observed in the case of 12 °C (Case D). However, there is no great difference observed when the indoor humidity of both cases is compared.
Figure 15 shows the dew condensation amount per month. The dew condensation amount increases with the decrease in the cold water temperature. It is expected to dehumidify as much as 80 L in August and the indoor hygrothermal environment can be predicted by the dew condensation on the panel.

Table 7 Calculation cases

	Method of cooling	Calculation of dew condensation	Supply water temperature
Case A	Air conditioner	-	-
Case B	Radiation panel system	×	7 deg.
Case C		○	
Case D		○	12 deg.

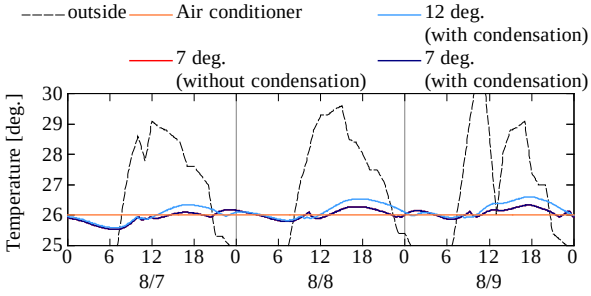

(1) Temperature

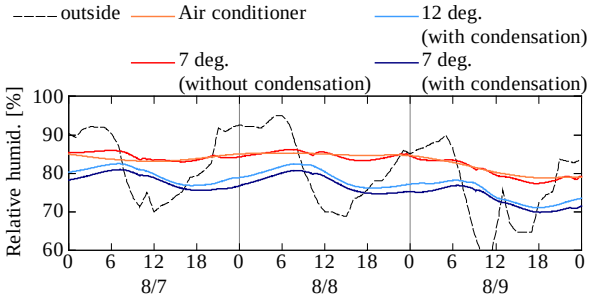

(2) Relative humidity

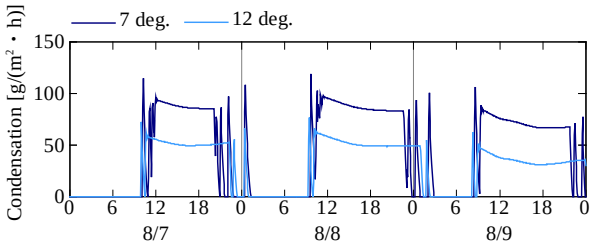

(3) Dew condensation

Figure 14 Effect of dew condensation

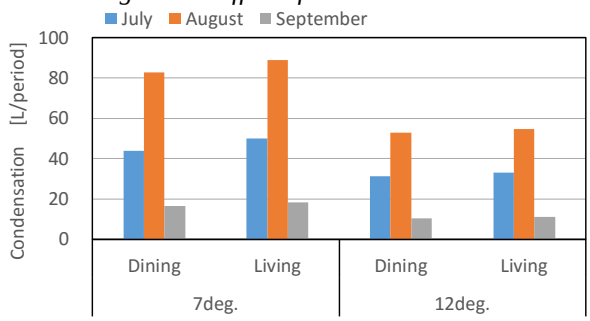

Figure 15 Dew condensation amount

CONCLUSIONS

In this study, we analyzed the hygrothermal environment of an experimental house installed with a stand-type radiation panel. Moreover, we calculated the parameters of the stand-type radiation panel by considering the convective heat transfer rate as well as the mutual

emission between the indoor surface and the two-dimensional heat movement between the pipes. We confirmed the high precision of our calculation by comparing with the actual value and the calculated value of the room temperature, relative humidity, surface temperature, and air conditioner load. Furthermore, we analyzed the effect of variation in the driving control method, cold-water temperature, and number of sheets on the indoor temperature. Finally, we discussed the determination of the indoor hygrothermal environment based on the dew condensation calculation. Sensitivity analyses of the radiation panel system provide the following results. 1) A radiation panel system can demonstrate sufficient ability even with low-grade heat source. 2) The efficiency of this system is improved by shielding the solar radiation from window. 3) The hygrothermal environment can be examined in detail by calculating the dew condensation on the radiation panel. 4) The hygrothermal environment in the summer is improved by dew condensation (dehumidification) on the radiation panel.

Symbols

A_f	: Cross section of pipe	[m^2]
C_f	: Thermal conductance from the fin surface	[W/(m^2·K)]
C_w	: Specific heat of water	[J/(kg·K)]
D	: Diameter of pipe	[m]
$F_{l,j}$	: View function for surface l to see surface	[-]
g	: Gravitational acceleration	[=9.8m/s^2]
Gr	: Grashof number	[-]
K_p	: Turbulent heat transfer coefficient in pipe	[W/(m^2·K)]
L_f	: Length of pipe	[m]
l	: Representative length	[m]
Nu	: Nusselt number	[-]
P	: perimeter of pipe	[m]
Pr	: Prandtle number	[-]
q_f	: Flow rate of supply water	[m^3/s]
Q	: Supply heat load of radiation panel	[W]
Ra	: Rayleigh number	[-]
R_b	: Thermal resistance per unit length from the inner surface of the pipe to the outer surface of the pipe	[m^2/(W·K)]
Re	: Reynolds number	[-]
S	: Surface area	[m^2]
t	: Thickness of pipe	[m]
T_s	: Surface temperature	[K]
T_m	: Temperature of each material	[K]
T_w	: Temperature in pipe	[K]
T_{ws}	: Temperature of supply water	[K]
ΔT_a	: Temperature difference between surface and air	[K]
V_w	: Amount of water in pipe	[m^3]
w	: Pitch of pipe	[m]
α_c	: Convective heat transfer coefficient	[W/(m^2·K)]
β	: expansion coefficient	[1/K]
ε	: Long wave emissivity of surface	[-]
η_f	: Fin efficiency	[-]
λ	: Thermal conductivity of fluid	[W/(m·K)]
λ_f	: Thermal conductivity of pipe	[W/(m·K)]
λ_w	: Thermal conductivity of water	[W/(m·K)]
ν	: dynamic coefficient of viscosity	[m^2/s]
ρ_w	: specific weight of water	[kg/m^3]

Acknowledgement

This study was supported by a Grant-in-Aid for Young Scientists (B) No.15K18170 from the Japan Society for the Promotion of Science (JSPS).

References

Watanabe, M. et al., 2004. Experimental study on evaluation of noise in the apartment, Architectural Institute of Japan convention academic lecture synopsis Collection, pp.105-106

Shioya, M et al., 2013. Study on heat performance of a ceiling slit panel unit for radiant cooling and heating, Architectural Institute of Japan, Environment engineer, AIJ, Vol.78 No.683, pp.31-37

Kim, J. et al., 2013. Study on the thermal characteristics on heating according to the location and figure of radiant heating panel, Architectural Institute of Japan, Environment engineer, AIJ, Vol.78 No.693, pp.859-864

Ozaki, A. et al., 2005. Temperature and humidity and heat load calculation of architecture that takes into account the heat and moisture - air coupling, Technical Papers of Annual Meeting of IBPSA-Japan, pp.19-26

Ozaki A., Watanabe T. et al., 1990, Heat and Mass Transfer at Outside Surface of Buildings – Wind Tunnel Tests of Heat and Mass Transfer on Horizontal Surfaces, Journal of Architecture, Planning and Environmental Engineering, Architectural Institute of Japan, No.407, p.11-25

Gebhart, B. 1959, A New Method for Calculating Radiant Exchanges, ASHRAE Transactions, Vol.6

Ozaki, A. et al., 2007. Driving Force and Diffusivity of Heat and Mass Transfer in Porous Materials, Technical Papers of Annual Meeting of IBPSA-Japan (7 pages)